Int J Clin Exp Med 2026;19(1):1-10
www.ijcem.com /ISSN:1940-5901/IJCEM0165908

Original Article

Bencao Shengji ointment promotes the healing of third-degree burn wounds in mice

Wenjiao Chen[1], Guoxin Liu[1], Zhongyuan Yang[2]

[1]Department of Dermatology, Wuhan Hankou Hospital, Wuhan, Hubei, PR China; [2]Department of Infectious Diseases, Tongji Hospital, Tongji Medical College and State Key Laboratory for Diagnosis and Treatment of Severe Zoonostic Infectious Disease, Huazhong University of Science and Technology, Wuhan, Hubei, PR China

Received May 9, 2025; Accepted December 2, 2025; Epub January 15, 2026; Published January 30, 2026

Abstract: Objectives: This study was conducted to verify the efficacy of Bencao Shengji ointment (BSO) in treating third-degree burn wounds in mice. Methods: In this study, a mouse model of third-degree burn wounds was established, and the mice were randomly divided into three groups. In Group A, a gel containing recombinant human epidermal growth factor was applied externally. In Group B, BSO was applied externally, and in Group C, Bencao Nursing Solution (BNS) was applied externally. The efficacy of traditional Chinese herbal medicine preparations was verified by observing and comparing burn wound healing, inflammatory reactions and scar formation in the skin of mice in the three groups from Day 4 to Day 60. Results: The wound healing in Groups B and C was better than that in Group A from Day 4 to Day 14. Compared with those in Group B and Group C, the degree of wound necrosis and extent of inflammatory reactions in Group A were greater. From Day 15 to Day 45, the scars that formed after healing in Group A were more obvious, and the scars that formed in Group B were the smallest. On the 60th day, the mice in Group B had the shallowest burn scars on their skin, whereas the mice in both Group A and Group C exhibited moderate to severe scar formation. Conclusions: BSO can better promote the healing of third-degree burn wounds and reduce the formation of scars.

Keywords: Bencao Shengji ointment, scar, third degree burn wounds

Introduction

Burns are acute tissue injuries that are caused by external factors such as heat, chemicals, electricity, or radiation, and they affect mainly the skin and mucous membranes [1, 2]. In severe cases, burns can also affect subcutaneous fat, muscles, and even bones. In clinical practice, burns are classified as first-degree, second-degree, and third-degree burns according to depth [3]. Among these burn types, third-degree burns (full-thickness skin burns) may temporarily prevent the sensation of pain due to the destruction of skin nerve endings, and these wounds appear as scabs and are difficult to heal, often requiring surgical intervention [4].

Pathologically, this type of injury manifests not only as immediate coagulative necrosis and microvascular embolism but also as a cascade inflammatory response, an oxygen free radical burst, and the release of many proinflammatory cytokines [1]. Although mild burns rarely pose a direct threat to life, transient and intense pain can continuously activate spinal dorsal horn neurons through A δ and C fibers, inducing central sensitization and leading to chronic neuropathic pain [5]. Moreover, the absence of the epidermal barrier increases transdermal water loss by more than 10-fold, causing electrolyte imbalance, hypoalbuminemia, and high metabolic status, significantly delaying wound healing [1, 6]. In the stage of scar hyperplasia, excessive activation of the TGF-β/Smad signaling pathway promotes the abnormal proliferation of myofibroblasts and disordered arrangement of collagen [7]. Ultimately, activation of this pathway results in the formation of hypertrophic scars or keloids, which not only restrict joint movement but also lead to disfigurement, causing anxiety, depression, and posttraumatic stress disorders, with a psychological disability rate of up to 34% [8, 9]. Additionally, scars that are produced in later stages can cause serious

https://doi.org/10.62347/NGXZ5818

inconvenience and psychological burden to patients [10]. Severe burns can lead to a sepsis cascade reaction 3-5 days after injury due to the breakdown of the natural immune barrier, displacement of the gut microbiota, and Th1/Th2 immune drift [1, 11]. This can easily result in secondary infections with pathogens such as *Pseudomonas aeruginosa* and *Staphylococcus aureus*, leading to fatal complications such as sepsis and multiple organ failure [12]. According to statistics, approximately 260,000 people worldwide die from burn-related infections each year, and approximately 15% of burn patients in China are hospitalized or die due to infections [13].

Traditional treatment involves "early scabbing, biological dressing coverage, and sequential skin grafting" [14]. Although topical sulfamethoxazole silver can inhibit infections with broad-spectrum bacteria, its cytotoxicity can delay epithelialization [15]. Repeated debridement can cause additional blood loss (loss of approximately 1-2% of circulating blood with each treatment) [2]. Although large medium-thick skin transplantation closes these wounds, the newly formed epithelium at the donor site is thin and prone to repeated rupture [7]. There is also a risk of skin necrosis and pigmentation, and the cost can reach 3,000 to 7,000 dollars per day, causing a heavy economic burden for patients in developing countries [16-19].

Topical preparations of traditional Chinese medicine are emerging as a new strategy for treating burns because of their "multicomponent, multitarget, holistic regulation" characteristics [20-22]. The main ingredients of Bencao Shengji ointment (BSO) include *Salvia miltiorrhiza*, *Ligusticum chuanxiong*, *cinnamon, purslane*, star anise, and licorice. BSO is formulated with the principle of "promoting blood circulation, removing blood stasis, and promoting muscle growth through detoxification" [23]. Tanshinone IIA reduces COX-2 expression by inhibiting NF-κB nuclear translocation, exerting analgesic effects similar those of NSAIDs [24]. Ligustrazine can upregulate VEGF-A and SDF-1α, promoting the homing of endothelial progenitor cells [25]. Cinnamaldehyde activates the TRPV1 channel to produce mild thermal stimulation, accelerating local blood flow perfusion [26]. Portulaca polysaccharides induce the polarization of M2 macrophages and inhibit excessive inflammation through the TLR4/MyD88 pathway [27]. Shikimic acid in star anise blocks STAT3 phosphorylation in fibroblasts in scars [28]. Glycyrrhetinic acid simulates the structure of glucocorticoids, reducing wound edema without the side effects of hormone-induced skin atrophy [29]. Network pharmacology analysis revealed that the core targets of BSO are enriched in the PI3K, Akt, HIF-1α, and Notch pathways, suggesting that BSO can achieve "scar-free healing" by regulating the stem cell microenvironment [21, 30-33].

This study established a mouse model of third-degree burn wounds, and the wound-healing effect of BSO compound herbal preparations were observed and verified, providing a theoretical basis for the application of these preparations in clinical practice.

Materials and methods

Experimental animals and drugs

Six-week-old specific pathogen-free (SPF) BALB/c male mice weighing approximately 20 g were purchased for experimentation (Zhuhai Baishitong Biotechnology Co., Ltd.). Three animals were housed in each cage and given free access to water and high-pressure sterilized commercial rations. The bedding was changed twice a week. These animals were carefully manipulated, always in the morning by the same researcher who received veterinary training and supervision. Drug A (recombinant human epidermal growth factor gel, Guilin Huanuo Co., Ltd., Guoyao Zhunzi s20020112), drug B (BSO, Hubei Guofutang Biomedical Technology Co., Ltd.), drug C (Bencao Nursing Solution, BNS, Hubei Guofutang Biomedical Technology Co., Ltd.) were administered to the mice. BSO and BNS are traditional Chinese medicine compound preparations with the same composition and different dosage forms, and they mainly include *Salvia miltiorrhiza*, *Ligusticum chuanxiong*, cinnamon, purslane, star anise, and licorice. This study followed the European Commission Directive 86/609/EEC for animal experiments (available at http://ec.europa.eu/environment/chemicals/lab_animals/legislation_en.htm). The animal experiments performed in the study were reviewed and approved by the Animal Experiment Ethics Committee of Wuhan Hankou Hospital.

Burn model establishment

After the mice were anesthetized with sodium pentobarbital, the hair on their backs was sha-

ved with a razor, and the backs were depilated with sodium sulfide until they were hairless. Water-soaked pieces of paper were placed on the backs of the mice (2.0 cm × 3.5 cm = 7.0 cm^2, accounting for 10% of the body surface area) to control the burn areas. Ethanol was dropped with a dropper onto the backs of the mice. The skin was soaked, and a lighter was used to ignite the ethanol. A stopwatch was used to measure the burn time, and the fire was extinguished with a damp cloth after 30 seconds, 40 seconds, 1 minute and 30 seconds, or 3 minutes. Third-degree burns were defined according to previous research [34]. During the treatment period, all the animals received closed and sterile bandages daily. During this process, 30 mg/kg tramadol hydrochloride was administered for analgesia.

Postburn care

A total of 21 mice with burns were randomly divided into three groups. Each group included 7 animals, and the animals were treated with drug A, B, or C. The wounds of Group A and B mice were treated with drugs A or B, respectively. The wounds in Group C were evenly sprayed with drug C. The drugs were administered twice a day, once in the morning and evening, within 7 days after the burn was established. The drugs were administered once a day beginning on the 8th day. One mouse with a burn that was not treated was used as a control.

Skin observation

On the designated analysis date, photos of the lesions were captured, and the various stages of the healing process, including necrosis, inflammation, and scarring, were macroscopically examined. On Days 3 and 60 after wound establishment, the animals were euthanized via injection with 100 mg/kg thiopental sodium, and wound healing, wound healing time, infection, and scarring during healing were analyzed.

Pathological examination

Changes in the surfaces of the wounds were recorded 3, 7, 14, 30, 45, and 60 days after burn injury. After the mice were sacrificed, the burn wound and the surrounding skin (approximately 0.5 cm) were removed, spread on filter paper, and then fixed in 10% formalin for subsequent pathological staining.

HE staining

Dewaxed paraffin sections were subjected to the following staining conditions, xylene I for 30 minutes, xylene II for 30 minutes, anhydrous ethanol I for 10 minutes, anhydrous ethanol II for 10 minutes, 95% alcohol for 5 minutes, 90% alcohol for 5 minutes, 80% alcohol for 5 minutes, and 70% alcohol for 5 minutes, followed by washing with distilled water. The slides were immersed in Harris hematoxylin for 8 minutes, rinsed with tap water, differentiated with 1% hydrochloric acid alcohol for a few seconds, rinsed with tap water for 10 minutes, returned to blue with PBS for 5 minutes, and rinsed with running water. The slides were then immersed in eosin staining solution for 2 minutes. Then, the sections were dehydrated and cleared under the following conditions, 95% alcohol I for 5 minutes, 95% alcohol II for 5 minutes, anhydrous ethanol I for 5 minutes, anhydrous ethanol II for 5 minutes, xylene I for 5 minutes, and xylene II for 5 minutes. Then, the sections were removed from the xylene, allowed to dry slightly, and then mounted with neutral paraffin. Microscopic examination, image acquisition, and analysis were then performed.

Ki67 staining

Xylene dewaxing was performed (2 times, 10 minutes each). The samples were hydrated by sequential incubation in gradient ethanol solutions (100%, 95%, 70%, and 50%) for approximately 3 minutes each. Finally, the samples were rinsed with PBS. Sodium citrate buffer (pH 6.0) was used for antigen retrieval. The sections were heated to 110°C in a pressure cooker, maintained for 15 minutes, and then allowed to cool naturally. Then, the slices were treated with 3% hydrogen peroxide (H_2O_2) for 10 minutes to block endogenous peroxidase activity. The cells were rinsed with PBS. The samples were then incubated in blocking solution supplemented with 3% BSA in PBS for 20 minutes to reduce nonspecific antibody binding. The Ki-67 primary antibody was diluted in PBS at a dilution ratio of 1:100. The mixture was incubated overnight at 4°C or at room temperature for 2 hours. The cells were rinsed 3 times with PBS for 5 minutes each. Then, an HRP-labeled anti-rabbit IgG secondary antibody was added,

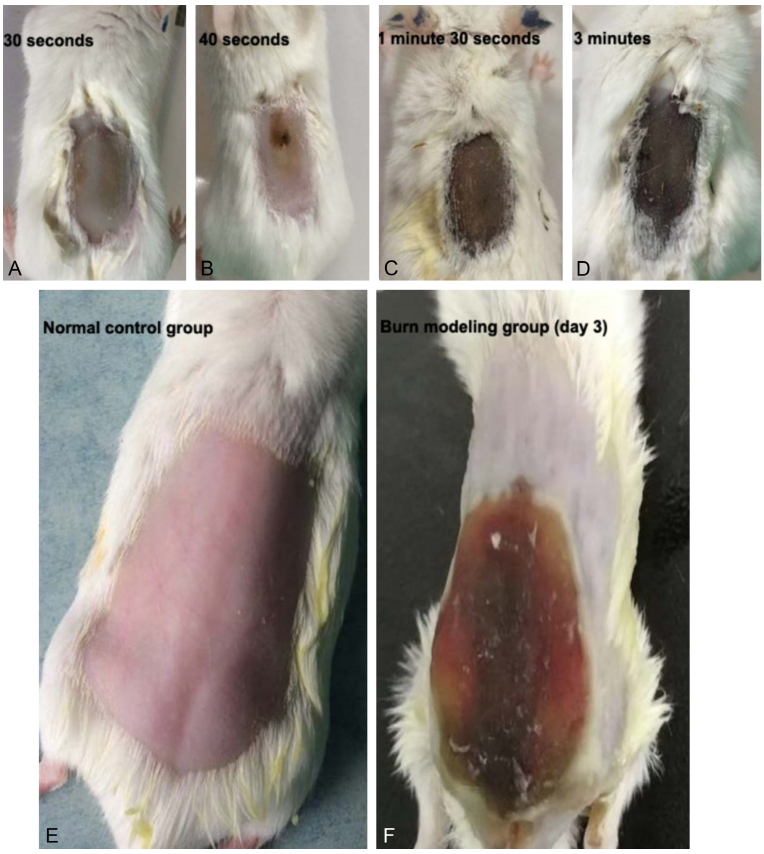

Figure 1. Determination of appropriate burn time and the early skin changes in burns. From left to right, burn for 30 seconds (A), 40 seconds (B), 1 Minutes 30 seconds (C) and 3 minutes (D). Normal mouse skin (E). Day 3 of third degree burn wound (F).

and the samples were incubated for 30 minutes. The cells were rinsed three times with PBS. DAB color reagent (3,3'-diaminobenzidine) was used for color development. The samples were incubated for 5 minutes, and the formation of brown precipitates was observed. The reaction was terminated with distilled water. Next, the cell nuclei were stained with hematoxylin for 2 minutes and rinsed with running water to develop the blue color. Then, the samples were dehydrated by sequential incubation with gradient ethanol solutions (70%, 95%, and 100%) for 2 minutes each. Xylene was used for transparency treatment. The slides were covered with neutral gum and a cover slip. Finally, the staining results were observed with an optical microscope.

Ki67 quantification

Following the same protocol, two dermatopathologists performed routine quantification of Ki67 staining and calculated the mean value [35]. To minimize interobserver variability, a consensus was reached following the assessment method. At least two randomly selected high-power fields in uniformly stained cases were evaluated. When Ki67 expression was heterogeneous, one area with the highest expression (hot spot) and one with the lowest expression (cold spot) were chosen. The average of these two regions was considered the final Ki67 score. Digital images were captured with a Roche slide scanner, and the mean value was obtained using a 20X microscope objective.

Statistical analysis

All data analysis in this study were performed by Student's t-test. SPSS 22.0 (Chicago, IL, USA) was used for data analysis. The difference of $P<0.05$ between the two groups was considered statistically significant.

Results

Establishment of a third-degree burn model in mice and early skin changes associated with burns

In the process of burn model establishment, we first observed the degree of skin burns on the backs of the mice subjected to modeling for 30 seconds (**Figure 1A**), 40 seconds (**Figure 1B**), 1 minute 30 seconds (**Figure 1C**) and 3 minutes (**Figure 1D**). Then, we determined that the appropriate duration for burn model establishment was 1 minute 30 seconds. At this time point, the burn affected the entire skin layer. Black eschar was visible, and the viability of the mice was acceptable. As shown in the following figure (**Figure 1F**), compared with those in the normal control group (**Figure 1E**), the mice in the burn model group presented obvious black necrotic areas on their backs, indicating an inflammatory state on Day 3.

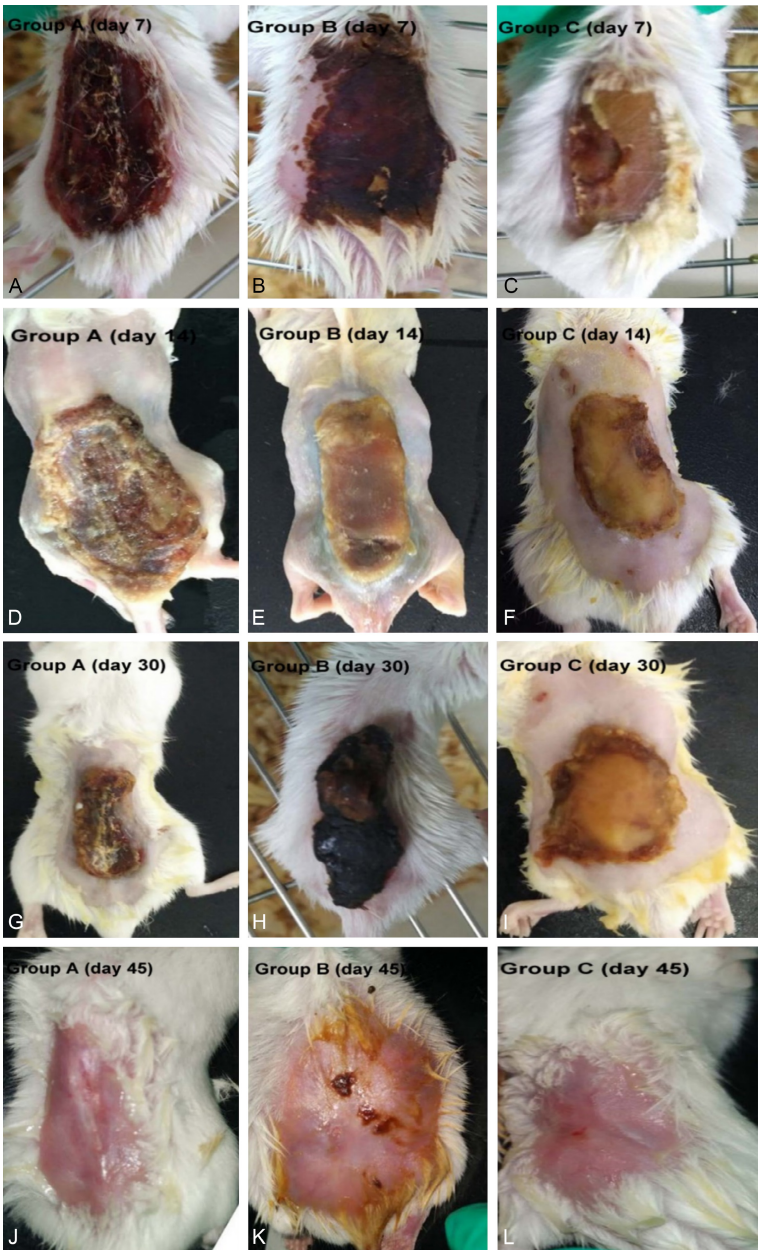

Figure 2. Back skin status of burned mice from 4 to 45 days. The back skin status from 4 to 7 days after burn in group A (A), group B (B) and group C (C). The back skin status from 8 to 14 days after burn in group A (D), group B (E) and group C (F). The back skin status at 30 days after burn in group A (G), group B (H) and group C (I). The back skin status at 45 days after burn in group A (J), group B (K) and group C (L).

Observation of the back skin of the mice during days 4-45 after burn injury

From 4-7 days after burn injury, the burned skin of the mice in Group A exhibited necrosis, and the original burned skin was damaged (**Figure 2A**). The skin of the mice in Group B was intact and covered with ointment, and no necrosis was detected when the material was collected (**Figure 2B**). The skin of the mice in Group C exhibited local skin peeling and necrosis (**Figure 2C**).

From 8-14 days after burn injury, the back skin of the mice in Group A became severely damaged and began to scab, with obvious redness and infection symptoms (**Figure 2D**). The skin of the mice in Group B was wrapped with ointment. Scabs were found during the sampling process, and the burned skin was intact (**Figure 2E**). A small part of the skin of the mice in Group C was damaged and began to scab (**Figure 2F**).

At 30 days after burn injury, the back skin of the mice in Group A had healed, with uneven crusts and signs of shedding (**Figure 2G**). The dorsal skin in Group B healed. The entire area was scabbed, and there were slight signs of shedding (**Figure 2H**). The skin on the backs of the mice in Group C healed slowly, and scabs started to form (**Figure 2I**).

At 45 days after burn, the wounds of the mice in each group had completely healed. The mice in Group B had slight scars (**Figure 2K**), and the mice in Groups A (**Figure 2J**) and C (**Figure 2L**) had obvious scars.

Observation of the back skin of the mice at 60 days after burn injury

After healing, the mice in Groups A and C (**Figure 3A** and **3C**) had moderate to severe scars on their backs, whereas the mice in Group B (**Figure 3B**) had mild scars.

Pathological evaluation

On the 3rd and 60th days after burn injury (**Figure 4**), pathological staining revealed disordered epidermal and dermal structures, infiltra-

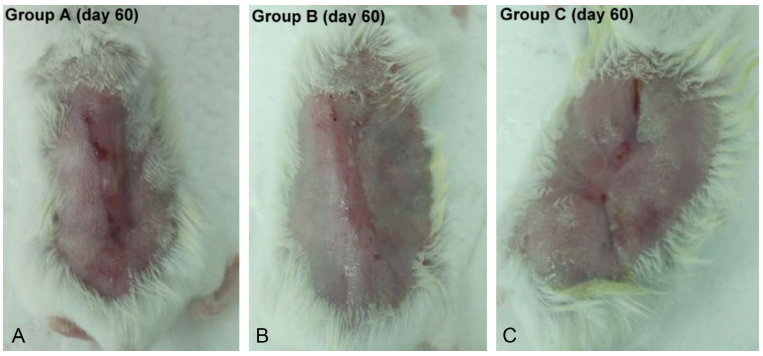

Figure 3. Back skin status of burned mice at 60 days. The back skin status at 60 days after burn in group A (A), group B (B) and group C (C).

tion of inflammatory cells into the dermis, dense and increased collagen fibers, and disordered arrangement in the untreated group. The skin morphology of mice in Group B had basically returned to normal, with clear epidermal and dermal structures and no abnormal increase in collagen fibers. Compared with the skin burn wounds in Group B, the skin burn wounds in Groups A and C exhibited obvious damage to the epidermal structure, a slight increase in the number of collagen fibers in the dermis, and the infiltration of inflammatory cells. This finding was consistent with the formation of scars in the gross images, which revealed that the untreated group had the most obvious scars, followed by Groups A and C, and Group B which had the smallest scars.

The results revealed that the Ki67-positivity rate of Groups B and C was significantly greater than that of Group A on Day 60, indicating that the healing and cell proliferation processes of the skin burn wounds in Groups B and C were better than those in Group A (**Figure 5**).

Discussion

The healing of burn wounds is a multifaceted and long process that depends on various repair mechanisms that depend upon the immune system. This regeneration occurs through three consecutive stages, namely, inflammation, proliferation, and remodeling, which may lead to scar formation [36, 37]. The local microenvironment, inflammatory reactions, infection, and malnutrition are considered the most important reasons for wound healing failure [38-41]. This study established a mouse model of third-degree burns, and during the course of the disease, there was an obvious inflammatory response that had a significant effect on the healing of burn wounds.

The treatment principles of traditional Chinese medicine are based mainly on syndrome differentiation and treatment [42]. The mechanism of treatment with traditional Chinese medicine includes promoting skin tissue growth, inhibiting the inflammatory response, inhibiting shock, and regulating collagen metabolism, thereby accelerating wound healing and inhibiting scar hyperplasia [43, 44]. Guided by the principles of traditional Chinese medicine syndrome differentiation and treatment, BSO uses *Salvia miltiorrhiza*, *Ligusticum chuanxiong*, cinnamon, purslane, star anise, and licorice as the core combination to achieve overall therapeutic effects through multitarget synergistic effects. Previous studies have confirmed that *Salvia miltiorrhiza* may promote the healing of burned skin by exerting anti-inflammatory effects, improving local wound microcirculation, and accelerating wound surface metabolism [21]. *Ligusticum chuanxiong* promotes the polarization of macrophages from a proinflammatory phenotype to a pro-healing phenotype, which can significantly accelerate wound closure. This is evident in the reduction of inflammation and the enhancement of angiogenesis and collagen deposition, indicating that *Ligusticum chuanxiong* has great potential for use in clinical applications related to skin healing [30]. Cinnamon accelerates wound healing by increasing the expression of insulin-like growth factor (IGF)-1, FGF-2, and vascular endothelial growth factor, thereby increasing cell proliferation, collagen synthesis, and re-epithelialization rates [45]. Purslane clears heat, relieves pain, exerts anti-inflammatory effects, and promotes repair [32]. Star anise has anti-inflammatory, antibacterial, and enhancing effects on cell proliferation, migration, and angiogenesis, and it is commonly used to treat infectious wounds [22, 46]. Licorice is the core drug of various traditional Chinese medicines that are used to promote wound repair and can have anti-inflammatory effects, promote blood circulation, regulate immunity, and facilitate wound repair [33].

In our study, the inflammatory response in the group treated with recombinant human epider-

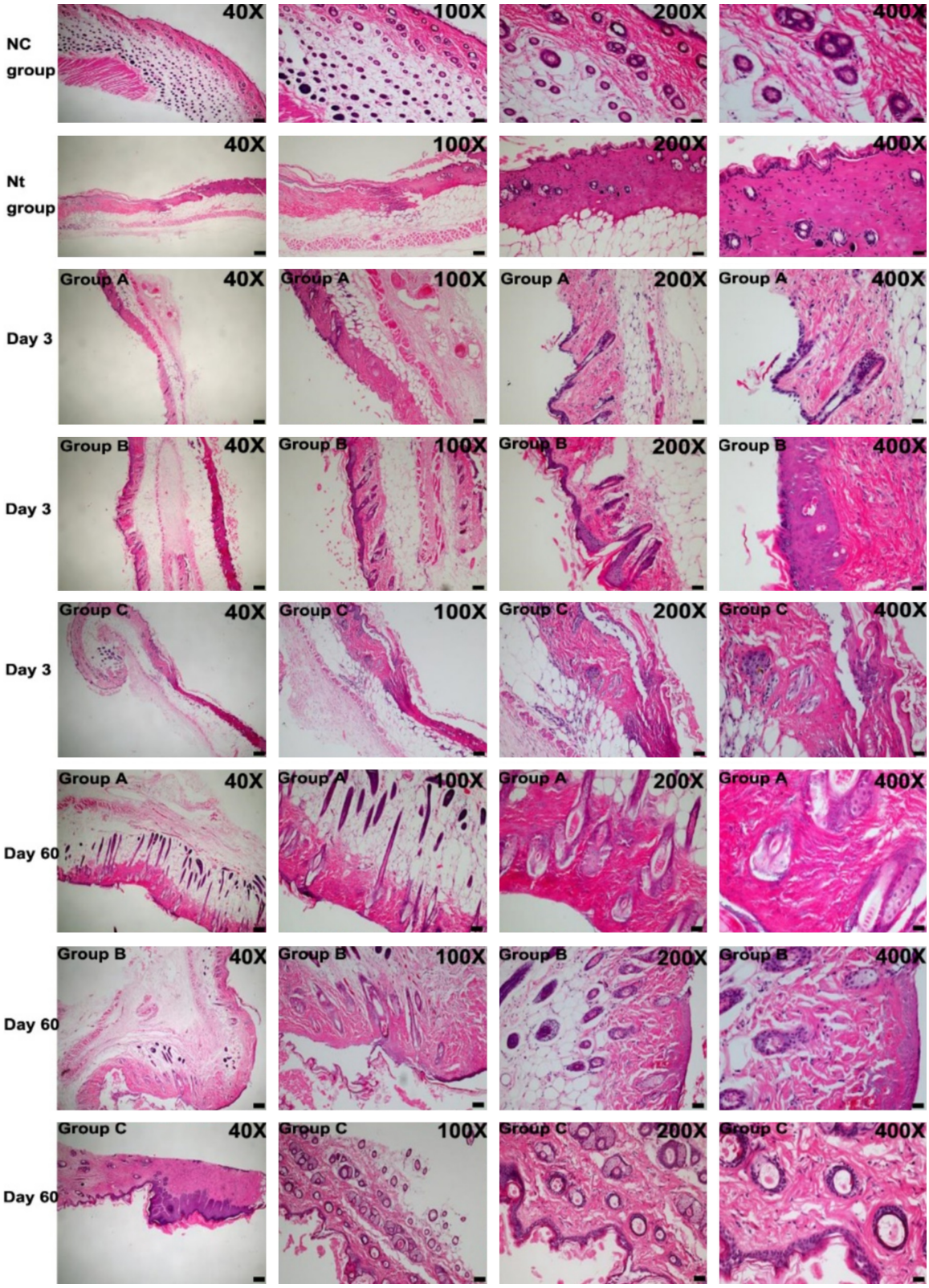

Figure 4. Pathological changes in mice after burn treatment. Pathological changes (HE staining). NC referred to the normal control group. Nt referred to the non-treatment group. The scale bar is 250 μm on 40X picture. The scale bar is 100 μm on 100X picture. The scale bar is 50 μm on 200X picture. The scale bar is 25 μm on 400X picture.

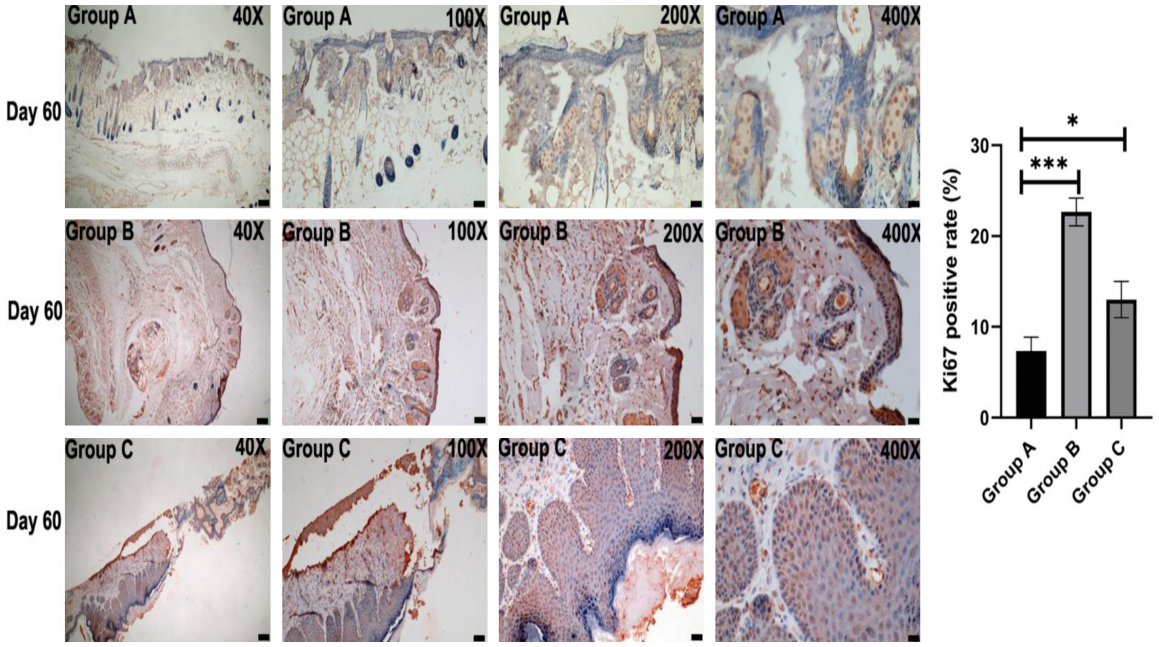

Figure 5. Immunohistochemistry results in mice after burn treatment. Expression and positivity rate of Ki67 in Group A, Group B and Group C. The scale bar is 250 μm on 40X picture. The scale bar is 100 μm on 100X picture. The scale bar is 50 μm on 200X picture. The scale bar is 25 μm on 400X picture. * represents $P<0.05$ and Group A compared to Group C. *** represents $P<0.001$ and Group A compared to Group B. Statistical significance was tested by Student's *t*-test.

mal growth factor was significant 8 to 14 days after burn injury, whereas the inflammatory response was milder in the BSO and BNS groups. During the same period, the wound healing rate of the BSO and BNS groups was faster than that of the human epidermal growth factor treatment group. These findings indicate that *Salvia miltiorrhiza*, *Ligusticum chuanxiong*, and cinnamon are involved in the anti-inflammatory repair process, significantly accelerating wound closure by reducing inflammation and enhancing angiogenesis. The anti-inflammatory, skin repair-promoting, and vascular regeneration-promoting effects of purslane, star anise, and licorice work synergistically with other components in BSO, resulting in superior effects of BSO on inflammation, healing, and scar formation.

At 45 and 60 days after burn injury, the scars in the BSO group were significantly lighter than those in the BNS and recombinant human epidermal growth factor treatment groups. Considering the significant correlation between the inflammatory response and scar formation, the results indicated BSO had better anti-inflammatory effects and reduced scar formation.

In this study, the pathological results of the BSO treatment group revealed that the inflammatory response was the lowest. The scars were the lightest, and the degree of healing was better. This finding was consistent with the condition of the lesion in the gross images. Ki67 is a nuclear protein that is present in the nucleus of proliferating cells. The rate of Ki67 positivity can reflect the degree of cell proliferation, and the higher Ki67 expression is, the stronger the cell proliferation activity is [47]. Our experiment confirmed that the Ki67 positivity rate was highest in the BSO treatment group, indicating that BSO exerted the best healing effect, which was consistent with previous experimental results [48].

There are several limitations in this study. The sample size of this study was limited, and the results will need to be fully verified with a larger sample size. In addition, the study focused mainly on a mouse model, and further clinical trials are needed.

In conclusion, experiments related to the use of skin treatments for third-degree burns revealed that the traditional Chinese herbal compound BSO could alleviate the inflammatory response, promote scar repair, and reduce scarring through a variety of mechanisms.

Disclosure of conflict of interest

None.

Address correspondence to: Dr. Zhongyuan Yang, Department of Infectious Diseases, Tongji Hospital, Tongji Medical College and State Key Laboratory for Diagnosis and Treatment of Severe Zoonostic Infectious Disease, Huazhong University of Science and Technology, No. 1095, Jiefang Avenue, Wuhan 430030, Hubei, PR China. Tel: +86-2783662391; Fax: +86-2783662391; E-mail: 1049446560@qq.com

References

[1] Jeschke MG, van Baar ME, Choudhry MA, Chung KK, Gibran NS and Logsetty S. Burn injury. Nat Rev Dis Primers 2020; 6: 11.

[2] Greenhalgh DG. Management of burns. N Engl J Med 2019; 380: 2349-2359.

[3] Monstrey S, Hoeksema H, Verbelen J, Pirayesh A and Blondeel P. Assessment of burn depth and burn wound healing potential. Burns 2008; 34: 761-769.

[4] Haruta A and Mandell SP. Assessment and management of acute burn injuries. Phys Med Rehabil Clin N Am 2023; 34: 701-716.

[5] Morgan M, Deuis JR, Frosig-Jorgensen M, Lewis RJ, Cabot PJ, Gray PD and Vetter I. Burn pain: a systematic and critical review of epidemiology, pathophysiology, and treatment. Pain Med 2018; 19: 708-734.

[6] Williams FN, Herndon DN and Jeschke MG. The hypermetabolic response to burn injury and interventions to modify this response. Clin Plast Surg 2009; 36: 583-596.

[7] Finnerty CC, Jeschke MG, Branski LK, Barret JP, Dziewulski P and Herndon DN. Hypertrophic scarring: the greatest unmet challenge after burn injury. Lancet 2016; 388: 1427-1436.

[8] Suca H, Coma M, Tomsu J, Sabova J, Zajicek R, Broz A, Doubkova M, Novotny T, Bacakova L, Jencova V, Kuzelova Kostakova E, Lukacin S, Rejman D and Gal P. Current approaches to wound repair in burns: how far have we come from cover to close? A narrative review. J Surg Res 2024; 296: 383-403.

[9] Dyster-Aas J, Willebrand M, Wikehult B, Gerdin B and Ekselius L. Major depression and posttraumatic stress disorder symptoms following severe burn injury in relation to lifetime psychiatric morbidity. J Trauma 2008; 64: 1349-1356.

[10] Waibel JS, Waibel H and Sedaghat E. Scar therapy of skin. Facial Plast Surg Clin North Am 2023; 31: 453-462.

[11] Nielson CB, Duethman NC, Howard JM, Moncure M and Wood JG. Burns: pathophysiology of systemic complications and current management. J Burn Care Res 2017; 38: e469-e481.

[12] D'Avignon LC, Chung KK, Saffle JR, Renz EM and Cancio LC; Prevention of Combat-Related Infections Guidelines Panel. Prevention of infections associated with combat-related burn injuries. J Trauma 2011; 71 Suppl 2: S282-289.

[13] Wang Y, Beekman J, Hew J, Jackson S, Issler-Fisher AC, Parungao R, Lajevardi SS, Li Z and Maitz PKM. Burn injury: challenges and advances in burn wound healing, infection, pain and scarring. Adv Drug Deliv Rev 2018; 123: 3-17.

[14] Legrand M, Depret F and Mallet V. Management of burns. N Engl J Med 2019; 381: 1188-1189.

[15] Atiyeh BS, Costagliola M, Hayek SN and Dibo SA. Effect of silver on burn wound infection control and healing: review of the literature. Burns 2007; 33: 139-148.

[16] Oryan A, Alemzadeh E and Moshiri A. Burn wound healing: present concepts, treatment strategies and future directions. J Wound Care 2017; 26: 5-19.

[17] Barillo DJ, Croutch CR, Barillo AR, Reid F and Singer A. Safety evaluation of silver-ion dressings in a porcine model of deep dermal wounds: a GLP study. Toxicol Lett 2020; 319: 111-118.

[18] Atiyeh B, Makkawi K and Beaineh P. Burn wounds and Enzymatic Debridement (ED)-past, present, and future. J Burn Care Res 2024; 45: 864-876.

[19] Bolton L. Burn debridement: are we optimizing outcomes? Wounds 2019; 31: 298-300.

[20] Bandopadhyay S, Mandal S, Ghorai M, Jha NK, Kumar M, Radha, Ghosh A, Prockow J, Perez de la Lastra JM and Dey A. Therapeutic properties and pharmacological activities of asiaticoside and madecassoside: a review. J Cell Mol Med 2023; 27: 593-608.

[21] Tian S, Guo L, Song Y, Yang H, Wang J, Qiao J, Wu X, Bai M and Miao M. Radix salvia miltiorrhiza ameliorates burn injuries by reducing inflammation and promoting wound healing. J Inflamm Res 2023; 16: 4251-4263.

[22] Chen ZC, Wu SS, Su WY, Lin YC, Lee YH, Wu WH, Chen CH and Wen ZH. Anti-inflammatory and burn injury wound healing properties of the shell of Haliotis diversicolor. BMC Complement Altern Med 2016; 16: 487.

[23] Zhang GB, Li QY, Chen QL and Su SB. Network pharmacology: a new approach for chinese herbal medicine research. Evid Based Complement Alternat Med 2013; 2013: 621423.

[24] Kwak HB, Sun HM, Ha H, Kim HN, Lee JH, Kim HH, Shin HI and Lee ZH. Tanshinone IIA suppresses inflammatory bone loss by inhibiting the synthesis of prostaglandin E2 in osteoblasts. Eur J Pharmacol 2008; 601: 30-37.

[25] Meng H, Guo J, Sun JY, Pei JM, Wang YM, Zhu MZ and Huang C. Angiogenic effects of the extracts from Chinese herbs: angelica and Chuanxiong. Am J Chin Med 2008; 36: 541-554.
[26] Rivera-Mancilla E, Al-Hassany L, Marynissen H, Bamps D, Garrelds IM, Cornette J, Danser AHJ, Villalon CM, de Hoon JN and MaassenVanDenBrink A. Functional analysis of TRPA1, TRPM3, and TRPV1 channels in human dermal arteries and their role in vascular modulation. Pharmaceuticals (Basel) 2024; 17: 156.
[27] Han P, Tian X, Wang H, Ju Y, Sheng M, Wang Y and Cheng D. Purslane (Portulacae oleracea L.) polysaccharide relieves cadmium-induced colonic impairments by restricting Cd accumulation and inhibiting inflammatory responses. Int J Biol Macromol 2024; 257: 128500.
[28] Gu Y, Zhang J, Zheng H, Qin Y, Zheng M, Hu Y and Xin J. Therapeutic effect of shikimic acid on heat stress-induced myocardial damage: assessment via network pharmacology, molecular docking, molecular dynamics simulation, and in vitro experiments. Pharmaceuticals (Basel) 2024; 17: 1485.
[29] Liu J, Xu Y, Yan M, Yu Y and Guo Y. 18betaglycyrrhetinic acid suppresses allergic airway inflammation through NF-kappaB and Nrf2/HO-1 signaling pathways in asthma mice. Sci Rep 2022; 12: 3121.
[30] Chu D, Chen J, Liu X, Liao A, Song X, Li Y, Yang L, Chen Z, Yu Z and Guo J. A tetramethylpyrazine-loaded hyaluronic acid-based hydrogel modulates macrophage polarization for promoting wound recovery in diabetic mice. Int J Biol Macromol 2023; 245: 125495.
[31] Anandhi P, Tharani M, Rajeshkumar S and Lakshmi T. Antibacterial activity of cinnamon and clove oil against wound pathogens. J Popul Ther Clin Pharmacol 2022; 28: e41-e46.
[32] Budiawan A, Purwanto A, Puradewa L, Cahyani ED and Purwaningsih CE. Wound healing activity and flavonoid contents of purslane (Portulaca grandiflora) of various varieties. RSC Adv 2023; 13: 9871-9877.
[33] Assar DH, Elhabashi N, Mokhbatly AA, Ragab AE, Elbialy ZI, Rizk SA, Albalawi AE, Althobaiti NA, Al Jaouni S and Atiba A. Wound healing potential of licorice extract in rat model: Antioxidants, histopathological, immunohistochemical and gene expression evidences. Biomed Pharmacother 2021; 143: 112151.
[34] Wu YC, Wu GX, Huang HH and Kuo SM. Liposome-encapsulated farnesol accelerated tissue repair in third-degree burns on a rat model. Burns 2019; 45: 1139-1151.
[35] Pons L, Hernandez-Leon L, Altaleb A, Ussene E, Iglesias R, Castillo A, Rodriguez-Martinez P, Castella E, Quiroga V, Felip E, Cirauqui B, Margeli M and Fernandez PL. Conventional and digital Ki67 evaluation and their correlation with molecular prognosis and morphological parameters in luminal breast cancer. Sci Rep 2022; 12: 8176.
[36] Shpichka A, Butnaru D, Bezrukov EA, Sukhanov RB, Atala A, Burdukovskii V, Zhang Y and Timashev P. Skin tissue regeneration for burn injury. Stem Cell Res Ther 2019; 10: 94.
[37] Burgess M, Valdera F, Varon D, Kankuri E and Nuutila K. The immune and regenerative response to burn injury. Cells 2022; 11: 3073.
[38] Wang Z, Qi F, Luo H, Xu G and Wang D. Inflammatory microenvironment of skin wounds. Front Immunol 2022; 13: 789274.
[39] Zhao Y, Zhao Y, Xu B, Liu H and Chang Q. Microenvironmental dynamics of diabetic wounds and insights for hydrogel-based therapeutics. J Tissue Eng 2024; 15: 20417314241253290.
[40] Kiley JL and Greenhalgh DG. Infections in burn patients. Surg Clin North Am 2023; 103: 427-437.
[41] Grada A and Phillips TJ. Nutrition and cutaneous wound healing. Clin Dermatol 2022; 40: 103-113.
[42] Dou Z, Xia Y, Zhang J, Li Y, Zhang Y, Zhao L, Huang Z, Sun H, Wu L, Han D and Liu Y. Syndrome differentiation and treatment regularity in traditional Chinese medicine for type 2 diabetes: a text mining analysis. Front Endocrinol (Lausanne) 2021; 12: 728032.
[43] Li FL, Wang GC and Wu BQ. Clinical application of traditional Chinese medicine powder in the treatment of acute and chronic wounds. Int Wound J 2023; 20: 799-805.
[44] Wang J, Hao L, Zhou X, He W and Hu M. Clinical application of traditional Chinese medicine moisture exposed burn ointment in the treatment of facial soft tissue defect. J Cosmet Dermatol 2022; 21: 2481-2487.
[45] Seyed Ahmadi SG, Farahpour MR and Hamishehkar H. Topical application of Cinnamon verum essential oil accelerates infected wound healing process by increasing tissue antioxidant capacity and keratin biosynthesis. Kaohsiung J Med Sci 2019; 35: 686-694.
[46] Wu J, Li X, Liang Y, Xiao Z and Su H. Protective effect of illicium verum extract on vascularization in rats with osteoporotic fracture. Altern Ther Health Med 2024; 30: 195-201.
[47] Li LT, Jiang G, Chen Q and Zheng JN. Ki67 is a promising molecular target in the diagnosis of cancer (review). Mol Med Rep 2015; 11: 1566-1572.
[48] Zhou Y, Zhang XL, Lu ST, Zhang NY, Zhang HJ, Zhang J and Zhang J. Human adipose-derived mesenchymal stem cells-derived exosomes encapsulated in pluronic F127 hydrogel promote wound healing and regeneration. Stem Cell Res Ther 2022; 13: 407.